Anomalies of liquid water at low temperature due to two types of hydrogen bonds

Yusong Tu[1,2] and Haiping Fang[1,*]
[1]*Shanghai Institute of Applied Physics, Chinese Academy of Sciences, P. O. Box 800-204, Shanghai 201800, China*
[2]*Graduate School of the Chinese Academy of Sciences, Beijing 100080, China*
(Received 19 October 2008; revised manuscript received 8 January 2009; published 30 January 2009)

It is believed that water anomalies are related to the hydrogen bonds between water molecules, but the relationship still remains a challenge. Here, by introducing two types of hydrogen bond—strong and weak, we successfully reproduce many liquid water anomalies, particularly the thermodynamic anomalies at supercooled temperature. We find that the exchange of strong and weak H bonds, which enhance the competition between the open and collapsed structures of liquid water, might be the key to those anomalies of supercooled liquid water. Our study is helpful in understanding the hydrogen bond structure in liquid water.

DOI: 10.1103/PhysRevE.79.016707 PACS number(s): 07.05.Tp, 61.20.Ja, 05.70.Jk, 64.60.My

Liquid water exhibits anomalous behaviors such as large heat capacity throughout the liquid range, expansion on freezing, and isothermal compressibility with a minimum. In recent years, the anomalies of water at low temperatures, such as dramatic increases of heat capacity, isothermal compressibility, and negative thermal expansivity as water is supercooled, have attracted special attention [1,2]. In experiments, the existence of the so-called no man's land (untouched by direct experiments) complicates investigations and leads to much controversy [1]. Theoretical models include simplified analytical models [3], lattice models [4], two-state models [5], field theoretical models [6], and models involving the competition of density and bond ordering [7].

Despite these efforts, the explanation of these anomalies of supercooled water, particularly their relationship with the behavior of hydrogen bonds, remains a challenge. Traditionally, in liquid water, each water molecule is thought to be H bonded to approximately four other water molecules in a tetrahedral arrangement [1]. In 2004, based on x-ray absorption spectroscopy, a "rings and chains" alternative model of liquid water was proposed [8]. In this model, at room temperature, 80% of the molecules of liquid water have one strong H-bonded O-H group and one non-, or only weakly, bonded O-H group at any instant, with the remaining 20% of the molecules being made up of H-bonded tetrahedrally coordinated molecules. This model was questioned in other experiments [9] and theoretical analyses [10], and so there have been hot debates [9–11].

In this study, we will focus on the hydrogen bonds and their significance for the anomalies of liquid water at low temperatures by introducing two types of H bond—the strong and the weak H bonds. Our study is based on Bol's waterlike model [12], in which tetrahedral local order is considered, and the strength of all H bonds is assumed to be the same. Bol's model is able to predict some anomalies, such as water maximal density [12], high heat capacity, thermal expansivity with zero value, and isothermal compressibility with a minimum. After the introduction of two types of H-bond strength, our model not only inherits the advantages of Bol's model, but is also successful in explaining water anomalies in the supercooled temperature region, which cannot be observed in Bol's model. We further find that the exchange of strong and weak H bonds may be the key to the anomalies of supercooled liquid water.

In Bol's model, water molecules are represented as hard spheres with four vectors assigned tetrahedrally in three-dimensional space (Fig. 1). We further assume that the H bonds have two types of strength. Explicitly, we assume a hard-sphere diameter σ, two orientation-dependent well depths $\varepsilon_{\mathrm{SHB}}, \varepsilon_{\mathrm{WHB}}$ ($|\varepsilon_{\mathrm{SHB}}| > |\varepsilon_{\mathrm{WHB}}|$), a well-width parameter f, and the pair interaction

$$U_{ij}(r_{ij},\theta_i,\theta_j) = \begin{cases} \infty, & r_{ij} < \sigma, \\ -\mathrm{sgn}(i)\mathrm{sgn}(j)\varepsilon_{\mathrm{SHB}}, & \sigma \leqslant r_{ij} < f\sigma \ \&\ |\theta_i| < \theta_s \ \&\ |\theta_j| < \theta_s, \\ -\mathrm{sgn}(i)\mathrm{sgn}(j)\varepsilon_{\mathrm{WHB}}, & \sigma \leqslant r_{ij} < f\sigma \ \&\ |\theta_i| < \theta_m \ \&\ |\theta_j| < \theta_m \ \&\ (|\theta_i| \geqslant \theta_s \| |\theta_j| \geqslant \theta_s), \\ 0 & \text{otherwise}, \end{cases} \tag{1}$$

where r_{ij} is the intermolecular distance, θ with molecular index i or j is the angle between the line connecting the centers of this pair of molecules and the nearest vector, $\mathrm{sgn}(i)$ and $\mathrm{sgn}(j)$ are equal to +1 or −1, depending on the sign associated with the vector involved, and the nearest vector is defined as the molecular vector with the smallest angle. This interaction provides two types of attractive H bond. Between a pair of molecules with $\sigma \leqslant r_{ij} < f\sigma$ and opposite-

*Corresponding author. fanghaiping@sinap.ac.cn

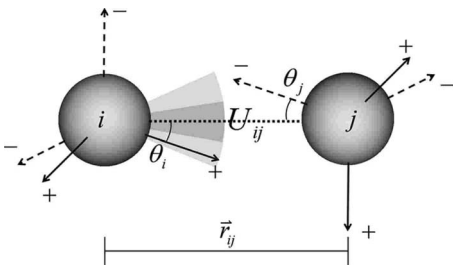

FIG. 1. Two water molecules with indices i and j separated by a distance r_{ij}. Each molecule consists of a hard sphere with four vectors pointing to the corners of a tetrahedron. A sign is associated with each of the four vectors of the molecules, two positive and two negative, representing two hydrogen atoms and the lone electronic pair of the water molecule. θ_i and θ_j are the smallest of the four angles between the vectors and the line connecting the centers of the two relevant molecules i and j.

sign nearest vectors, a strong H bond is established if these two nearest vectors fall into the small-angle region ($\theta_i < \theta_s$ and $\theta_j < \theta_s$), and a weak bond is formed if both nearest vectors fall into the preset-angle region (less than θ_m) and at least one of them is outside that small-angle region (larger than θ_s). When $\theta_s = \theta_m$ and $\varepsilon_{SHB} = \varepsilon_{WHB} = \varepsilon_{HB}$, our model returns to Bol's model.

Our model has six parameters. We set $\sigma = 1$, $f = 1.1$, $\theta_m = 27°$, and $\varepsilon_{HB} = -1$, consistent with Bol's model [12], and $\varepsilon_{SHB} = \varepsilon_{HB} = -1$, $\theta_s = 12°$, and $\varepsilon_{WHB} = -0.68$. These last two parameters characterize the relationship between strong and weak H bonds, and in this study, they are about half of θ_m and ε_{SHB}, respectively. Numerically, we find that other choices close to those two values do not change the conclusion. Additionally, all energies and temperatures will be reported in reduced units, and normalized to the strength of the optimal H bond, $H^* = H\varepsilon_{HB}^{-1}$ and $T^* = k_B T \varepsilon_{HB}^{-1}$. Similarly, all distances are scaled by the length of an idealized hard-sphere diameter, $V^* = V\sigma^{-3}$, and $P^*V^* = PV/|\varepsilon_{HB}|$.

Monte Carlo (MC) simulations were performed in the *NPT* ensemble [13], Simulations were performed in a cubic box with standard periodic boundary conditions for molecule number $N = 300$ at constant $P^* = 0.3$. After the first 10^7 MC steps with random initial configurations, we collect data over the next 10^7 MC steps. The ensemble averages use 40 independent runs for each state point, and the errors are estimated by calculating the variance with the block average [13].

Both Bol's and our model display maximal density occurring at $T^* = 0.145$ in Bol's model and 0.1225 in our model [Fig. 2(a)]. Bol's model presents a relatively faint maximum, and this maximum becomes very clear in our model. Also, an inflection point of molar volume is observed at $T_w^* \approx 0.108$ in our model, at which temperature the numbers of strong and weak H bonds are equal [Fig. 3(b)].

Figure 2(b) shows the dependence of heat capacity (C_P) on temperature. Our model captures the main characteristic of liquid water. An almost constant heat capacity holds at high temperatures, and an anomalous maximum occurs at T_w^*, which is consistent with the inflection-point temperature of the molar volume. We note that C_P of liquid water increases sharply as the temperature decreases and reaches its

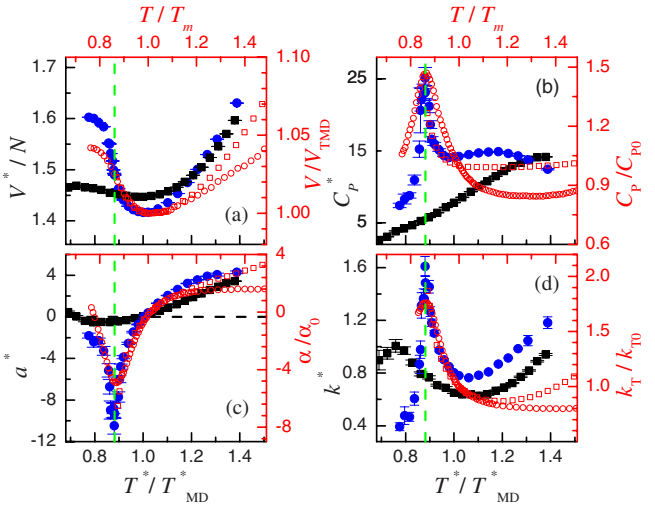

FIG. 2. (Color online) Temperature dependence of (a) molar volume, (b) heat capacity, (c) thermal expansivity, and (d) isothermal compressibility. Simulation results [Bol's model (■) and the present model (●)] use the left and bottom axes. Experimental results (liquid water (□) and tellurium (○) [2]) adopt the right and top axes. The simulation data are shown as a function of T/T^*_{MD}, where T^*_{MD} was the temperature at the maximal density of the liquid water ($T^*_{MD} = 0.1225$ in our model and 0.145 in Bol's model), and the temperature in the experimental results is normalized to the melting points T_m of liquid water ($T_m = 0$ °C) and tellurium (449.5 °C), respectively. C_{P0}, α_0, and k_0 are the relevant values at T_m, and the volume is scaled to its value at the volume minimum V_{TMD} (density maximum). Dashed green vertical lines correspond to $T_w^* \approx 0.108$ and $T_p = -38$ °C.

maximal value at $T = T_p$ [Fig. 2(b)]. The behavior of our prediction for $T^* > T_w^*$ is consistent with the experimental observation for liquid water for $T > T_p$. In contrast, only a monotonic increase of heat capacity is obtained from Bol's model.

Liquid water presents its abnormal expansion below 4 °C. In our simulations, our model predicts a sharp valley

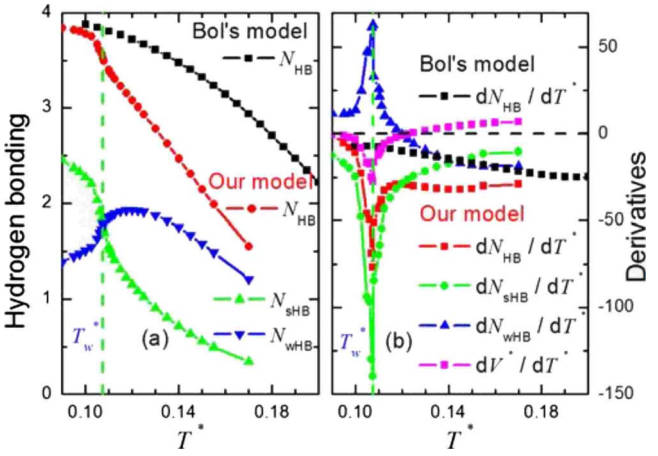

FIG. 3. (Color online) (a) Temperature dependence of the average H-bond numbers per molecule and (b) their derivatives together with the derivative of molar volume. The green dashed vertical line at T_w^* coincides with the critical temperature of these extrema as shown in Fig. 2.

of thermal expansivity (α) at T_w^* [Fig. 2(c)], the same temperature as for the C_p^* maximum. This is consistent with the experimental observation of the sharp decrease of α until T_p in liquid water. But for Bol's model, the change of α_P^* is rather slight. In addition, both models exhibit temperatures at $\alpha_P^*=0$ consistent with their temperatures at the density maximum [see Fig. 2(a)].

In Fig. 2(d), we can observe a maximal value of the isothermal compressibility (k) for both models. However, the temperature of the maximal k^* value, $T^*=0.11$, in Bol's model is different from the temperature at the minimal α^* value. In contrast, in the present model, the temperature of the maximal k^* value, T_w^*, is consistent with the critical temperature for the sharp C_p^* peak and the α^* valley. We note that, in liquid water, as the temperature decreases to T_p, there is a sharp increase of isothermal compressibility, and the critical temperature is the same as that of both the heat capacity and thermal expansivity. It is clear that the behavior of our model for $T^*>T_w^*$ is quite consistent with the behavior of liquid water for $T>T_p$. In addition, one observes k^* minima, at $T^*=0.16$ in Bol's model, $T^*=0.13$ in our model, consistent with the k^* minimum at $\sim$46.5 °C in liquid water (at atmospheric pressure) [1], all of which are larger than the temperatures of the density maxima.

Figure 3 shows the temperature dependence of the average numbers of H bonds per molecule and their derivatives. Bol's model presents a smooth decrease of the average numbers of H bonds per molecule as temperature increases. In contrast, one can see an initial increase of the number of weak H bonds, N_{WHB}, in the low-temperature region in the present model, and then it levels off before decreasing. The number of strong H bonds, N_{SHB}, decreases monotonically as the temperature increases. Remarkably, at the critical temperature T_w^* for several anomalies, $N_{\mathrm{SHB}}=N_{\mathrm{WHB}}$; before it, $N_{\mathrm{WHB}}<N_{\mathrm{SHB}}$ and after it, $N_{\mathrm{WHB}}>N_{\mathrm{SHB}}$.

In Bol's model, with increase of temperature, the number of H bonds decreases, which suggests the occurrence of partial collapse or more compact structures. The competition between the opposing effects of increasing temperature, structural collapse, and thermal expansion leads to some anomalies of liquid water such as maximal density, thermal expansivity with zero value, and isothermal compressibility with a minimum. The present model inherits these advantages of Bol's model.

The introduction of strong and weak H bonds makes the structural collapse more sensitive to the temperature, enhancing the ability for structural transformation. In particular, at the temperature T_w^* where $N_{\mathrm{WHB}}=N_{\mathrm{SHB}}$, there exist peaks of heat capacity and isothermal compressibility, and a dip of the thermal expansivity. For $T^*<T_w^*$, $N_{\mathrm{WHB}}<N_{\mathrm{SHB}}$ suggests that the model liquid is more structured and more low-density-like (open structure), while for $T^*>T_w^*$, $N_{\mathrm{WHB}}>N_{\mathrm{SHB}}$ indicates that it is less structured and more high-density-like (partially collapsed structure). In Fig. 3(b), we show the derivatives of the numbers of H bonds per molecule in both models. One can see a clear peak for the weak H bonds and clear dips for the strong H bonds and the total number $N_{\mathrm{WHB}}+N_{\mathrm{SHB}}$ at $T^*=T_w^*$. These extrema cause clear inflection points of both strong and weak H bonds at $T^*=T_w^*$. In a word, the greatest exchange of strong and weak H bonds in response to temperature change occurs at $T^*=T_w^*$. Also, this exchange suggests a close competition at $T^*=T_w^*$ between the open and collapsed structures, which is quite consistent with the experimental observations on confined water with comparable concentrations of these two types of local structure at $T\approx-48$ °C [14]. The resulting local structural change brings about a direct effect—the inflection point of molar volume [Fig. 3(b)]. Thus, it is the exchange of the strong and weak H bonds, suggesting a dramatic change of the local structures, that leads to the extrema of heat capacity, isothermal compressibility, and thermal expansivity (i.e., the peaks and dips in Fig. 2), which is consistent with the experimental observations on liquid water at $T\geqslant T_p$. We note that the region with lower temperature is experimentally unreachable and there are no direct data for bulk water within this region [1,2].

Liquid tellurium has only one kind of atom, which has a quite different structure from water. However, as seen in Fig. 2, the thermodynamic properties of liquid tellurium are surprisingly similar to the predictions from the present model at low temperatures. Recently, the structure of liquid tellurium was characterized by interactions with two possible length scales, that is, the Te-Te covalent bond and a second, longer-distance interaction [2]. The observations imply that a two-level interaction may be the key to understanding liquid water at a low temperature. Our observation may present a direct understanding of the hydrogen bond structure in liquid water.

To summarize, we have developed a simplified model of liquid water by introducing strong and weak H bonds in Bol's waterlike model. Remarkably, by introduction of strong and weak H bonds, the present model greatly improves Bol's predictions on the behavior of liquid water at low temperature. The predicted existence of the extrema of heat capacity, isothermal compressibility, and thermal expansivity at the same critical temperature T_w^* are consistent with the available experimental data on liquid water [14]. The success of the present model lies in the exchange of the strong and weak H bonds. As the temperature changes, one observes inflection points of both the numbers of strong and weak H bonds and of all H bonds at the critical temperature T_w^*.

The strong and weak H bonds defined here could be different from those described by Nilsson *et al.* [9]. Conventionally, the strengths of H bonds are distributed continuously depending on the orientation and distance between a pair of water molecules. From a coarse-grained perspective, the H bonds can be approximated through potentials of constant strength for a first-step approximation, like Bol's model, two-strength potentials, like our model, and more complex potentials. The success of our model shows that two-strength H bonding is capable of capturing the primary characteristics of liquid water.

We thank Professor Anders Nilsson, Professor Teresa Head-Gordon, and Professor George Ewing for their helpful discussions, and Dr. H. Kanno for providing the data. This work was supported by the Chinese Academy of Sciences, the National Science Foundation of China under Grant Nos.

10674146 and 10825520, the National Basic Research Program of China under Grant Nos. 2007CB936000 and 2006CB933000, and Shanghai Supercomputer Center of China.

APPENDIX: SIMULATION DETAILS AND CALCULATIONS OF THERMODYNAMIC QUANTITIES

In the *NPT*-ensemble Monte Carlo simulations [13], an aggregation-volume-bias (AVB) algorithm (AVBMC2 in the original paper) [15] and configurational-bias (CB) method [15] with multiple orientations were applied to circumvent difficulties in getting away from bottlenecks or traps in phase space caused by the presence of "bonded" configurations, especially down to the temperature of supercooled water. Verlet neighbor lists [16] were used to speed up search pairs.

At each successive step, four types of MC movement were performed with a random sequence according to the relevant frequencies. The random sequence includes randomly visiting twice each of N particles for (i) translational and rotational movements and (ii) translational and rotational movements with CB multiple orientations, (iii) visiting $N \times 10\%$ particles for AVB movements with CB multiple orientations, and (iv) performing volume rescaling once. At each MC step, the frequencies of each type of movement are kept and all elements of this sequence are reshuffled randomly. The maximum displacement and size of volume interchange were adjusted to give about 50% acceptance for trial movements, and for the configurational-bias method, the number of multiple orientations was set to 5.

Mechanical averages such as the enthalpy (H^*) and volume (V^*) are computed in the standard way, as the average of those quantities over the course of the simulation. The heat capacity C_p^*, the isothermal compressibility α^*, and the thermal expansion coefficient k^* are computed from the fluctuations:

$$C_p^* = C_p/k_B = (\langle H^{*2}\rangle - \langle H^*\rangle^2)/NT^{*2},$$

$$\alpha^* = (\langle V^*H^*\rangle - \langle V^*\rangle\langle H^*\rangle)/(T^{*2}\langle V^*\rangle),$$

$$k^* = (\langle V^{*2}\rangle - \langle V^*\rangle^2)/(T^*\langle V^*\rangle).$$

[1] P. G. Debenedetti, J. Phys.: Condens. Matter **15**, R1669 (2003); T. Loerting and N. Giovambattista, *ibid.* **18**, R919 (2006); O. Mishima and Y. Suzuki, Nature (London) **419**, 599 (2002); O. Mishima and H. E. Stanley, *ibid.* **396**, 329 (1998); P. G. Debenedetti, *ibid.* **392**, 127 (1998); R. Ludwig, Angew. Chem., Int. Ed. **45**, 3402 (2006); C. A. Angell, Science **319**, 582 (2008).

[2] A. Angell, Nat. Nanotechnol. **2**, 396 (2007); H. Kanno, H. Yokoyama, and Y. Yoshimura, J. Phys. Chem. B **105**, 2019 (2001).

[3] P. H. Poole, F. Sciortino, T. Grande, H. E. Stanley, and C. A. Angell, Phys. Rev. Lett. **73**, 1632 (1994); T. M. Truskett, P. G. Debenedetti, S. Sastry, and S. Torquato, J. Chem. Phys. **111**, 2647 (1999); C. A. Jeffery and P. H. Austin, *ibid.* **110**, 484 (1999).

[4] C. J. Roberts and G. D. Pablo, J. Chem. Phys. **105**, 658 (1996).

[5] E. G. Ponyatovsky and V. V. Sinitsyn, Physica B **265**, 121 (1999).

[6] M. Sasai, J. Chem. Phys. **93**, 7329 (1990).

[7] H. Tanaka, Phys. Rev. Lett. **80**, 5750 (1998).

[8] P. Wernet *et al.*, Science **304**, 995 (2004).

[9] T. Head-Gordon and M. E. Johnson, Proc. Natl. Acad. Sci. U.S.A. **103**, 7973 (2006); J. D. Smith, C. D. Cappa, K. R. Wilson, B. M. Messer, R. C. Cohen, and R. J. Saykally, Science **306**, 851 (2004); Y. A. Mantz, B. Chen, and G. J. Martyna, J. Phys. Chem. B **110**, 3540 (2006).

[10] M. Sharma, R. Resta, and R. Car, Phys. Rev. Lett. **95**, 187401 (2005); M. V. Fernandez-Serra and E. Artacho, *ibid.* **96**, 016404 (2006); D. Prendergast and G. Galli, *ibid.* **96**, 215502 (2006); R. Bukowski, K. Szalewicz, G. C. Groenenboom, and A. v. d. Avoird, Science **315**, 1249 (2007).

[11] J. D. Eaves, J. J. Loparo, C. J. Fecko, S. T. Roberts, A. Tokmakoff, and P. L. Geissler, Proc. Natl. Acad. Sci. U.S.A. **102**, 13019 (2005); M. Leetmaa *et al.*, J. Chem. Phys. **129**, 084502 (2008); T. Tokushima *et al.*, Chem. Phys. Lett. **460**, 387 (2008).

[12] W. Bol, Mol. Phys. **45**, 605 (1982); J. Slovák and I. Nezbeda, *ibid.* **101**, 789 (2003).

[13] D. Frenkel and B. Smit, *Understanding Molecular Simulation: From Algorithms to Applications* (Academic Press, San Diego, 2002), p. 525.

[14] F. Mallamace, M. Broccio, C. Corsaro, A. Faraone, D. Majolino, V. Venuti, L. Liu, C.-Y. Mou, and S.-H. Chen, Proc. Natl. Acad. Sci. U.S.A. **104**, 424 (2007).

[15] B. Chen and J. I. Siepmann, J. Phys. Chem. B **105**, 11275 (2001); J. I. Siepmann and D. Frenkel, Mol. Phys. **75**, 59 (1992).

[16] L. Verlet, Phys. Rev. **159**, 98 (1967).